

## Field Test of Thermoelectric Generators at Bottle Rock Geothermal Power Plant

Kewen Li<sup>1,2</sup>, Geoffrey Garrison<sup>3</sup>, Michael Moore<sup>3</sup>, Yuhao Zhu<sup>2</sup>, Changwei Liu<sup>1,2</sup>, Jay Hepper<sup>3</sup>, Larry Bandt<sup>3</sup>, Roland Horne<sup>1</sup>, and Susan Petty<sup>3</sup>

<sup>1</sup>Stanford University, Stanford, CA94305, USA

<sup>2</sup>China University of Geosciences, Beijing

<sup>3</sup>AltaRock Energy, Inc.

kewenli@stanford.edu

**Keywords:** thermoelectric generator system, direct power generation, thermoelectric effect, thermal efficiency

### ABSTRACT

One of the great challenges to using thermoelectric generators (TEG) for power generation is large-scale utilization. It is difficult to manufacture TEG systems even at the scale of a few kilowatts (KW). There have been many reports on laboratory experiments measuring TEG power output at different flow rates of water, different temperatures, and other different conditions, but there have been few field tests utilizing geothermal wells. To this end, we designed a geothermal-TEG apparatus that has a six-layer modularized design to allow expanded power production. After demonstrating the TEG's performance in the laboratory, we tested the apparatus in the field at a well located in the Bottle Rock geothermal field in The Geysers, CA, USA. The whole six-layer TEG device could generate about 500 W electricity with a temperature difference of about 152 °C between the hot and cold fluid manifolds, while each TEG chip could generate about 3.9 W. The steam pressure at the inlet of the TEG apparatus was about 122 psi, close to the wellhead pressure of 125 psi. After optimizing the field infrastructure, the six-layer TEG device could generate electricity without any leak at the wellhead pressure of 125 psi and the temperature over 176 °C (349 °F). The field test of the six-layer TEG device at Bottle Rock geothermal power plant was considered successful, and plans have begun to design and build a TEG device that could produce power up to 20 KW.

### 1. INTRODUCTION

Technology using thermoelectric generators (TEG) can transform thermal energy into electricity directly by using the Seebeck effect. TEG electricity generation technology has many advantages such as compactness, quietness, and reliability because there are no moving parts. Many studies have been conducted to improve the power performance and decrease the cost or self-energy consumption in recent years (Ahmadi Atouei et al., 2017; Araiz et al., 2017; Atouei et al., 2018; Boonyasri et al., 2017; Cao et al., 2018; Chen et al., 2017; Deasy et al., 2017; Demir and Dincer, 2017b, 2017a; Huang et al., 2018; Huang and Xu, 2017; Kane et al., 2016; Kim et al., 2017, 2016, 2018; Lee and Lee, 2018; Lekbir et al., 2018; Li et al., 2019; Lu et al., 2017; Lv et al., 2017; Negash, 2017; Remeli et al., 2016; Sajid et al., 2017; Twaha et al., 2016; Wang et al., 2014).

There have been many other earlier studies, both numerical and experimental, on TEG power generation technology (Angeline et al., 2019; Bijukumar et al., 2018; Deasy et al., 2017; He et al., 2019; Höglblom and Andersson, 2016; Lan et al., 2018; Ming et al., 2017; Tu et al., 2017; Yu and Zhao, 2007; Zhang, 2016; Zhao et al., 2018).

One of the challenges to using TEGs for power generation is large-scale utilization (Li et al., 2019) because it can be difficult to manufacture a TEG system even at the scale of a few kilowatts (KW). Previous studies have reported on numerical modeling and the laboratory experiments conducted to measure the power output at different flow rates of water, different temperatures, and other different conditions, but there have been few field tests utilizing geothermal wells.

Accordingly, we designed a six-layer TEG apparatus that could be installed with modularized units, with the ultimate objective of building a 20 KWe system. Such a system with a layered structure can be expanded in power. We tested the TEG apparatus at a geothermal well in the Bottle Rock geothermal field in The Geysers, CA, USA, after conducting experiments in the laboratory. The field test results are presented in this paper. A simple cost analysis was conducted, and the results showed that the cost of TEGs is less than that of solar photovoltaic (PV) panels if availability and capacity factor is considered.

### 2. FIRST FIELD TEST

We first conducted a pilot field test with a five-layer lab-scale TEG apparatus after the successful experiments in our laboratory. The five-layer TEG apparatus could be fit in a small box and was delivered to the geothermal well pad located at Bottle Rock (see Figure 1). In order to connect the five-layer TEG lab apparatus to the geothermal well head system, pipes, adapters, and manifolds were constructed to adapt the different pipe fittings between the TEG lab apparatus and the geothermal well, as shown in Figure 2 and Figure 3.

The field test was run on July 27, 2019 after the installation of the five-layer TEG apparatus. It was not possible to control the inlet pressure and steam flow rate into the apparatus because no pressure control valve (PCV) was installed. The five-layer TEG apparatus

Li et al.

leaked due to the high pressure and high temperature. It was not possible to measure any power output. We learned a lot from this field test even though the output could not be obtained.



**Figure 1: The five-layer TEG apparatus could be fit in a small box and was moved to the geothermal well pad in Bottle Rock, California, USA.**

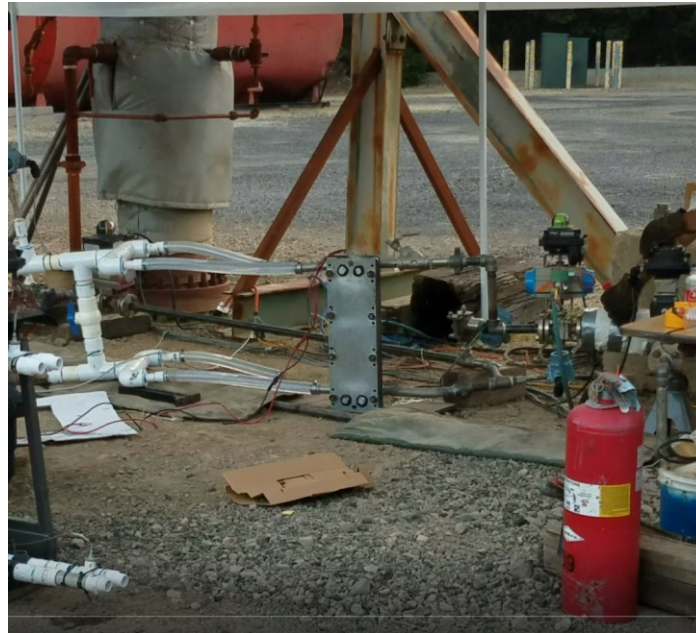


**Figure 2: The geothermal well head at Bottle Rock, California, USA (pipes and manifolds were adapted to connect to the five-layer TEG lab apparatus).**



**Figure 3: The five-layer TEG lab apparatus, ready to be tested at the geothermal well at Bottle Rock, California, USA, July 2019.**

### 3. SECOND FIELD TEST

We shipped the leaked five-layer lab-scale TEG apparatus back to our laboratory and conducted a diagnosis after disassembling it. It was found that the reason for the leaks was because the sealing structure was good for high temperature but not good for high pressure. We redesigned the structure and made a new six-layer-TEG apparatus (see Figure 4). The new six-layer-TEG apparatus has a dimension of 75 cm (length) X 24 cm (width) X 18 cm (height). The TEG device can withstand high pressure better, without leak, if the pressures on the cold and hot sides of the TEG chips are approximately equal to each other.

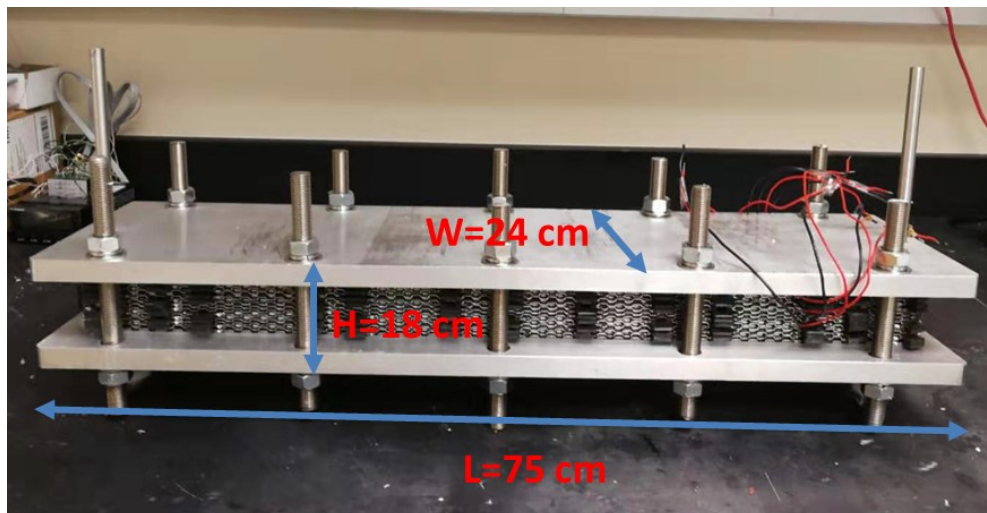


**Figure 4: The photo of the modified six-layer-TEG device.**

Figure 5 shows the schematic and the flow configuration of the six-layer-TEG apparatus used for the field tests. High temperature steam flows into the TEG device from lower right side and out from the lower left side. Cold water flows in the opposite direction. The heat exchange between the cold and hot sides of the TEG modules could be enhanced by directing the hot and cold flow in a countercurrent way.

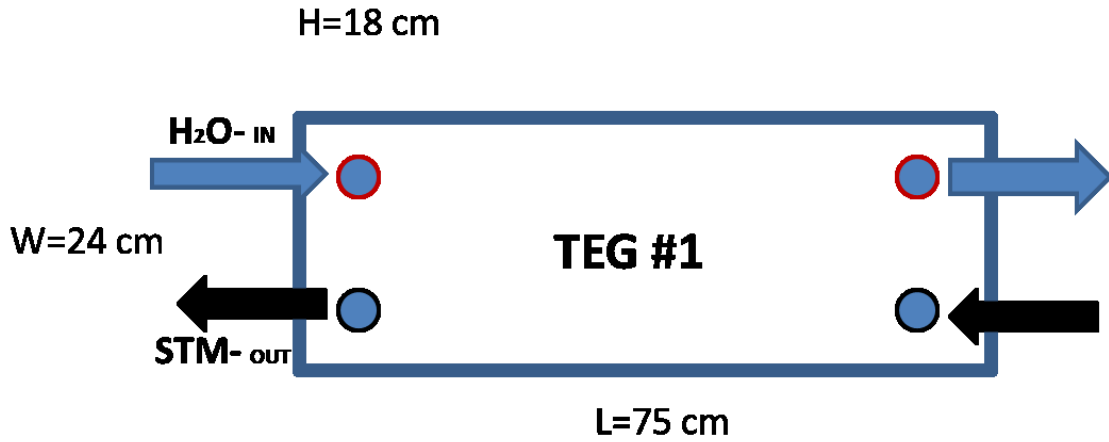
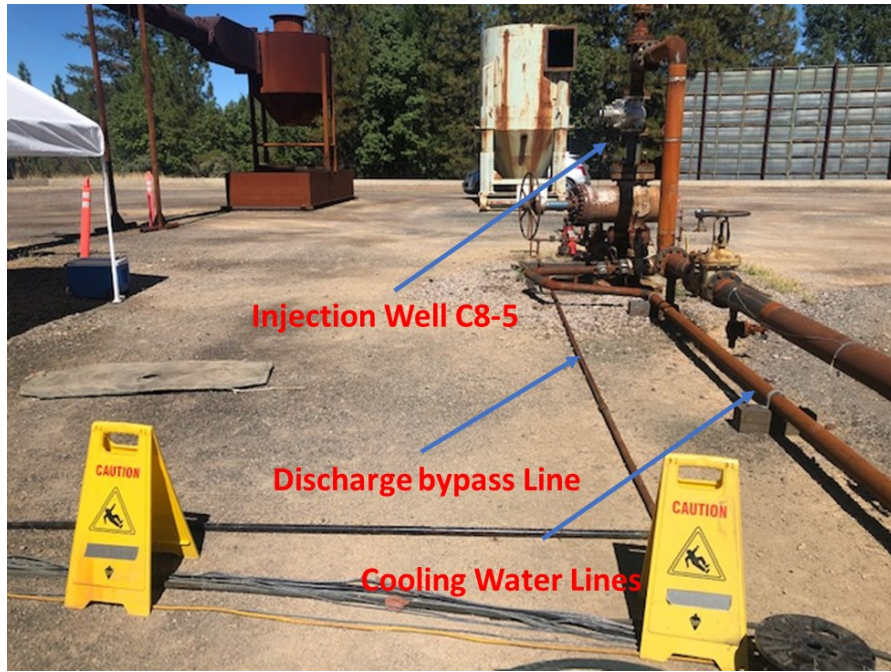


**Figure 5: The schematic and the flow configuration of the six-layer-TEG device.**

The instruments and the arrangement near the geothermal production well head for the second field test are shown in Figure 6a. A pressure control valve (PCV) was installed this time in order to control the inlet pressure and steam flow rate into the new six-layer-TEG apparatus. With the PCV, we could test the TEG apparatus at different inlet pressures and determine the specific pressure at which the TEG apparatus started to leak. The power output as a function of steam pressure or steam flow rate could be measured. The pipes near the geothermal injection well are shown in Figure 6b. The cold water supply and the control panel for sampling data near the geothermal wells are shown in Figure 6c.



(a) The instruments near the geothermal production well head



(b) The piping arrangement near the geothermal injection well



(c) Cold water supply and the control panel for sampling data near the geothermal wells

**Figure 6: Photos of the geothermal well and the piping network at the Bottle Rock facility**

Figure 7 shows the piping network from the geothermal well at the Bottle Rock facility. A steam by-pass line in parallel with the six-layer-TEG apparatus was installed in order to protect the TEG device if any unexpected situation occurred. The pressure and the flow rate of the cold water flowing through the cold side could also be controlled. The purpose was to balance the pressure on the cold and hot sides of the TEG chips in order to allow the TEG device withstand higher pressure without leaking through the seals.

The schematic and the flow configurations were the same as for the first field test. The main difference in the second field test was that the pressure control valve (PCV) was installed. With the PCV, the power output as a function of steam pressure or steam flow rate could be measured.

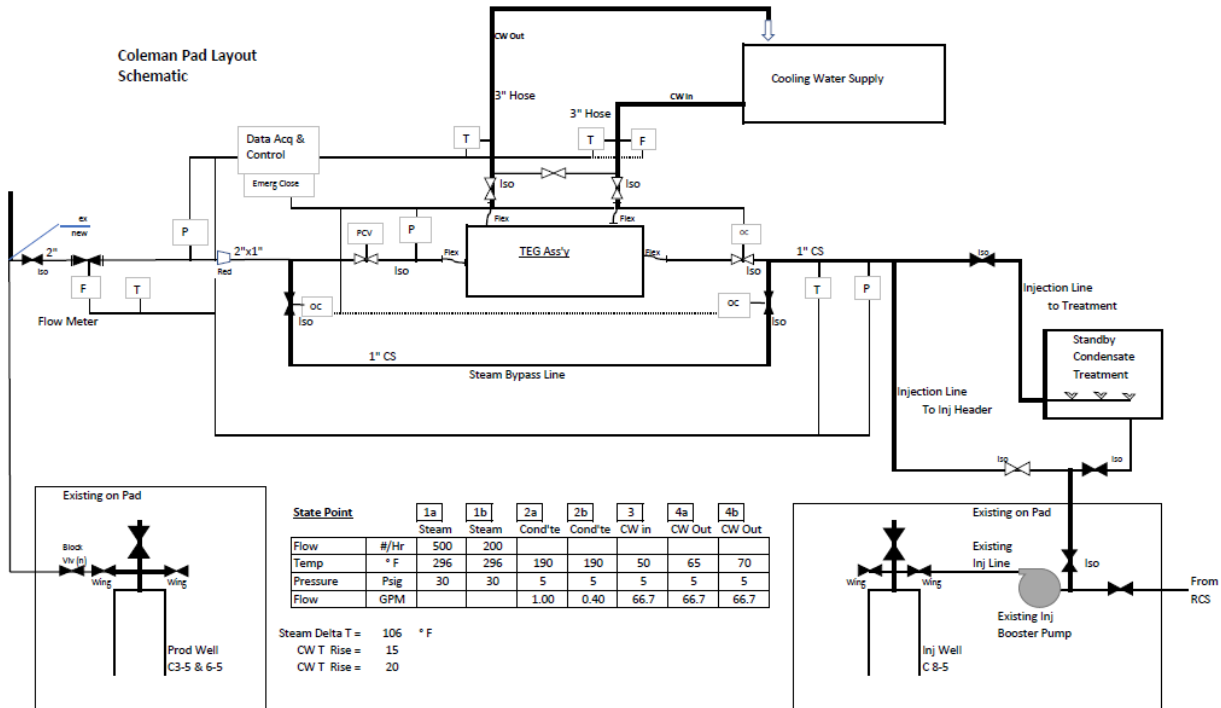


**Figure 7: The schematic and the arrangement of the six-layer-TEG apparatus with the piping network from the geothermal well at the Bottle Rock facility**

The new six-layer TEG apparatus was installed at Bottle Rock geothermal field for testing, as shown in Figure 8. The geothermal well (Coleman 3-5) has been shut down and had not been in production for a very long time. It took us over five hours to warm up the geothermal producer (Coleman 3-5). We then conducted the tests and measured the power output at different steam pressures (or steam flow rate) using the steam from this geothermal production well and at different pressures of cold water (or water flow rate). The field test began on September 27, 2019 and ended on September 29, 2019.

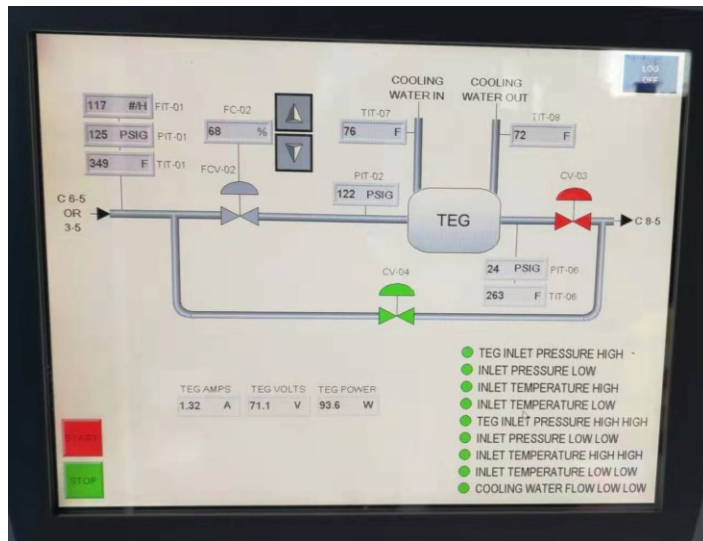


**Figure 8: The new six-layer TEG apparatus installed for field test at Bottle Rock geothermal field.**

The new six-layer TEG apparatus had no leak when the inlet steam pressure was less than 100 psi and leaked a little when fully open to the maximum pressure from the geothermal production well. The steam pressure at the inlet of the six-layer TEG apparatus was about

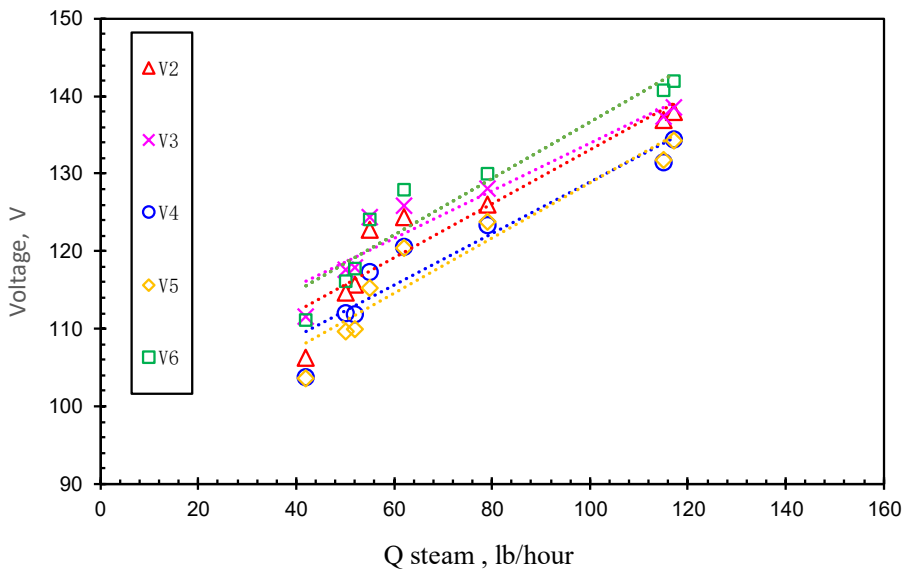
122 psi, close to the wellhead pressure of 125 psi at the geothermal producer. The apparatus stopped leaking when the pressure of the cold water was increased to about 80 psi.

A data acquisition system was developed to record the values of pressure, temperature, and flow rate at both inlet and outlet on cold and hot sides of the TEG apparatus. A typical screen shot of the data acquisition system is shown in Figure 9. The new six-layer TEG device could generate about 93.6 W per layer (about 500 W total) without any leak at the wellhead pressure of 125 psi and the temperature over 176 °C (349 °F).



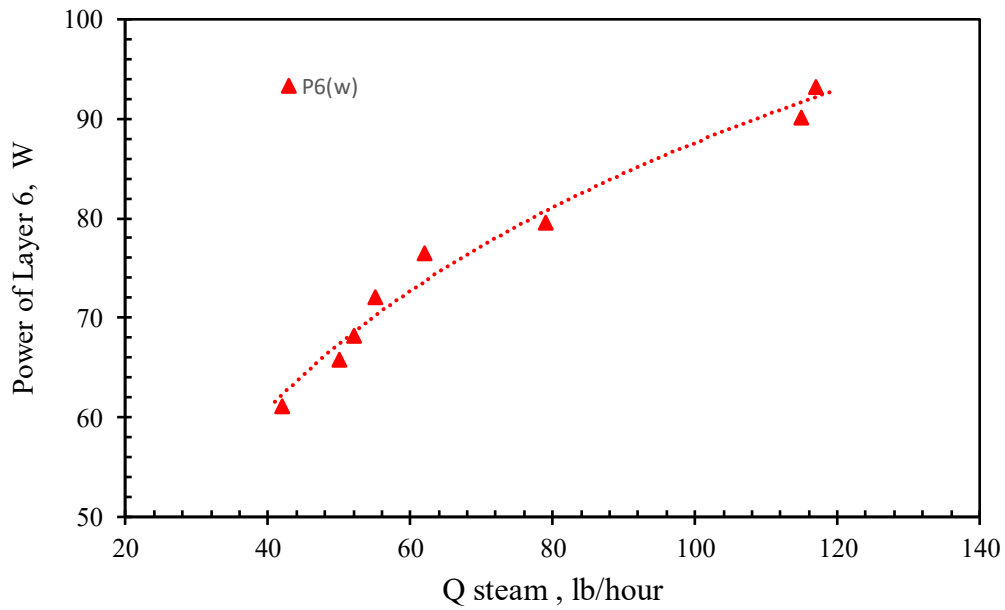
**Figure 9: The screen shot of the power output and other parameters measured using the modified six-layer TEG apparatus at Bottle Rock geothermal field.**

Figure 10 shows the voltage measured from each layer of the apparatus except for the first layer (V1, which had failed). According to the results, one layer with 24 chips could generate a voltage from 120 V to about 140 V per layer at the pressure of 125 psi and temperature over 176 °C (349 °F). The most important feature is that the values of the voltage from each layer did not vary significantly, which follows the trend of the experimental results as we presented in the paper at the 2019 Stanford Geothermal Workshop (Li et al., 2019). Layer 6 had the highest voltage.



**Figure 10: Voltage measured from each layer as a function of steam flow rate.**

We measured the power of a single layer (Layer 6) separately, and the results are shown in Figure 11. Layer 6 (with 24 chips) could generate about 93.6 W and each chip could generate about 3.9 W. The power increased with the steam flow rate. This also follows the trend of the laboratory results as we presented in the paper at the 2019 Stanford Geothermal Workshop (Li et al., 2019).



**Figure 11: Power vs. steam flow rate measured from the sixth layer**

The values of the voltage from each layer did not vary significantly, as shown in Figure 10. We know that the power is directly proportional to the voltage (Li et al., 2019). The total power for the six-layer TEG apparatus was then estimated. The results are shown in Figure 12. The total estimated power reached about 560 W at a steam flow rate of 120 lb. per hour.

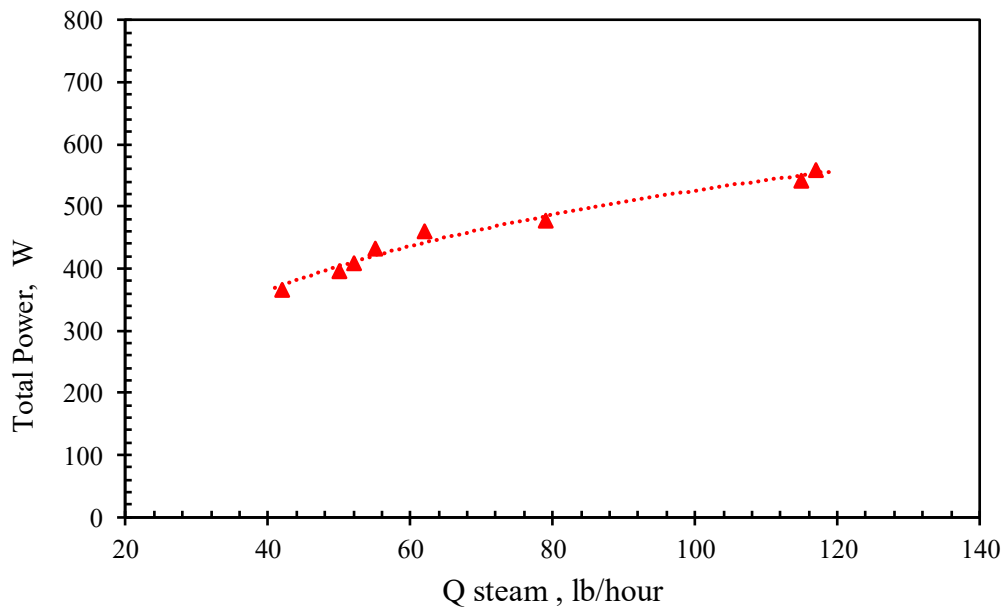


**Figure 12: The total power estimated for the six-layer TEG apparatus in field tests**

The volumetric power density of the TEG apparatus was estimated based on the field test results. A device with a physical volume of 50 cubic meter could generate about 1 MW of electric power, which is very attractive.

Based on these data, the second field test of the six-layer TEG apparatus conducted at the Bottle Rock geothermal facility in California, USA was considered to have been successful.

**4. PRELIMINARY COST ANALYSIS**

According to the initial analysis of the results of the second field test, it was estimated that the cost of per KW would be around \$13,900. The total cost of the 20 KW TEG would be around \$280,000, using the TEG chips deployed in the six-layer test device, and the volume

of a 20 KW TEG device would be around 1 m<sup>3</sup>. These costs are very attractive compared with solar photovoltaic (PV) panels. Based on the data reported by White (2019), the average cost of solar PV panels in 2019 in the United States is about \$3050 per KW. The capacity factors of solar PV are between 10 and 25%, and they average about 20%, due to nights and cloudy days (Li et al., 2015). The cost of solar PV panels is greater than that of TEGs if capacity factor is considered. TEG devices have a capacity factor of ~99%, and so the net cost of solar PV panels at a capacity factor comparable to a TEG system would be about \$15,250/kW. At a scale larger than 20 KW, the cost of per KW TEG could be less than \$13,900. TEG devices may also be cost competitive with binary geothermal power generation technology because TEG does not need turbines and does not need the binary fluid.

## 5. CONCLUSIONS

According to our field test results, the following conclusions may be drawn:

- (1) At a steam flow rate of 120 lb/hour, one layer (Layer 6 with 24 chips) could generate about 93.6 W, and each chip could generate around 3.9 W electricity with a temperature difference of 152 °C between the cold and hot fluid manifolds.
- (2) The voltage and power output of each layer is almost the same, which makes the delivering of the electricity to the load easier, more uniform, and more stable.
- (3) The effects of flow rate on the voltage and power output have been tested at the Bottle Rock geothermal facility in California, USA. The voltage and power also increase with the water flow rate on both cold and hot sides, but not linearly.
- (4) The second field test of the six-layer TEG apparatus conducted at Bottle Rock was successful and the results had a trend similar to the data measured in the laboratory.
- (5) A TEG system with a volume of 50 m<sup>3</sup> could generate about 1 MW electric power. Such a unit is comparable in size to a 1 MW diesel-powered generator and could supply a thousand homes.

## ACKNOWLEDGEMENT

This research was conducted with financial support from California Energy Commission (EPC-16-036), the contributions of which are gratefully acknowledged.

## REFERENCES

- Ahmadi Atouei, S., Ranjbar, A.A., Rezaia, A., 2017. Experimental investigation of two-stage thermoelectric generator system integrated with phase change materials. *Appl. Energy* 208, 332–343. <https://doi.org/10.1016/j.apenergy.2017.10.032>
- Angeline, A.A., Asirvatham, L.G., Hemanth, D.J., Jayakumar, J., Wongwises, S., 2019. Performance prediction of hybrid thermoelectric generator with high accuracy using artificial neural networks. *Sustain. Energy Technol. Assessments* 33, 53–60. <https://doi.org/10.1016/j.seta.2019.02.008>
- Araiz, M., Martínez, A., Astrain, D., Aranguren, P., 2017. Experimental and computational study on thermoelectric generators using thermosyphons with phase change as heat exchangers. *Energy Convers. Manag.* 137, 155–164. <https://doi.org/10.1016/j.enconman.2017.01.046>
- Atouei, S.A., Rezaia, A., Ranjbar, A.A., Rosendahl, L.A., 2018. Protection and thermal management of thermoelectric generator system using phase change materials: An experimental investigation. *Energy* 156, 311–318. <https://doi.org/10.1016/j.energy.2018.05.109>
- Bijukumar, B., Kaushik Raam, A.G., Ganesan, S.I., Nagamani, C., 2018. A Linear Extrapolation-Based MPPT Algorithm for Thermoelectric Generators under Dynamically Varying Temperature Conditions. *IEEE Trans. Energy Convers.* 33, 1641–1649. <https://doi.org/10.1109/TEC.2018.2830796>
- Boonyasri, M., Jamradloedluk, J., Lertsatitthanakorn, C., Therdyothin, A., Soponronnarit, S., 2017. Increasing the Efficiency of a Thermoelectric Generator Using an Evaporative Cooling System. *J. Electron. Mater.* 46, 3043–3048. <https://doi.org/10.1007/s11664-016-5142-9>
- Cao, Q., Luan, W., Wang, T., 2018. Performance enhancement of heat pipes assisted thermoelectric generator for automobile exhaust heat recovery. *Appl. Therm. Eng.* 130, 1472–1479. <https://doi.org/10.1016/j.applthermaleng.2017.09.134>
- Chen, J., Li, K., Liu, C., Li, M., Lv, Y., Jia, L., Jiang, S., 2017. Enhanced efficiency of thermoelectric generator by optimizing mechanical and electrical structures. *Energies* 10, 1–15. <https://doi.org/10.3390/en10091329>
- Deasy, M.J., Baudin, N., O’Shaughnessy, S.M., Robinson, A.J., 2017. Simulation-driven design of a passive liquid cooling system for a thermoelectric generator. *Appl. Energy* 205, 499–510. <https://doi.org/10.1016/j.apenergy.2017.07.127>
- Demir, M.E., Dincer, I., 2017a. Development and heat transfer analysis of a new heat recovery system with thermoelectric generator. *Int. J. Heat Mass Transf.* 108, 2002–2010. <https://doi.org/10.1016/j.ijheatmasstransfer.2016.12.102>
- Demir, M.E., Dincer, I., 2017b. Performance assessment of a thermoelectric generator applied to exhaust waste heat recovery. *Appl. Therm. Eng.* 120, 694–707. <https://doi.org/10.1016/j.applthermaleng.2017.03.052>
- He, H., Wu, Y., Liu, W., Rong, M., Fang, Z., Tang, X., 2019. Comprehensive modeling for geometric optimization of a thermoelectric generator module. *Energy Convers. Manag.* 183, 645–659. <https://doi.org/10.1016/j.enconman.2018.12.087>
- Höglblom, O., Andersson, R., 2016. A simulation framework for prediction of thermoelectric generator system performance. *Appl. Energy* 180, 472–482. <https://doi.org/10.1016/j.apenergy.2016.08.019>

- Huang, Q., Li, X., Zhang, G., Zhang, J., He, F., Li, Y., 2018. Experimental investigation of the thermal performance of heat pipe assisted phase change material for battery thermal management system. *Appl. Therm. Eng.* 141, 1092–1100. <https://doi.org/10.1016/j.applthermaleng.2018.06.048>
- Huang, S., Xu, X., 2017. A regenerative concept for thermoelectric power generation. *Appl. Energy* 185, 119–125. <https://doi.org/10.1016/j.apenergy.2016.10.078>
- Kane, S.N., Mishra, A., Dutta, A.K., 2016. Investigation of aluminum heat sink design with thermoelectric generator, in: *Journal of Physics: Conference Series*. <https://doi.org/10.1088/1742-6596/755/1/011001>
- Kim, H.S., Liu, W., Ren, Z., 2017. The bridge between the materials and devices of thermoelectric power generators. *Energy Environ. Sci.* 10, 69–85. <https://doi.org/10.1039/c6ee02488b>
- Kim, T.Y., Kwak, J., Kim, B. wook, 2018. Energy harvesting performance of hexagonal shaped thermoelectric generator for passenger vehicle applications: An experimental approach. *Energy Convers. Manag.* 160, 14–21. <https://doi.org/10.1016/j.enconman.2018.01.032>
- Kim, T.Y., Negash, A.A., Cho, G., 2016. Waste heat recovery of a diesel engine using a thermoelectric generator equipped with customized thermoelectric modules. *Energy Convers. Manag.* 124, 280–286. <https://doi.org/10.1016/j.enconman.2016.07.013>
- Lan, S., Yang, Z., Chen, R., Stobart, R., 2018. A dynamic model for thermoelectric generator applied to vehicle waste heat recovery. *Appl. Energy* 210, 327–338. <https://doi.org/10.1016/j.apenergy.2017.11.004>
- Lee, W., Lee, J., 2018. Development of a compact thermoelectric generator consisting of printed circuit heat exchangers. *Energy Convers. Manag.* 171, 1302–1310. <https://doi.org/10.1016/j.enconman.2018.06.063>
- Lekbir, A., Hassani, S., Ab Ghani, M.R., Gan, C.K., Mekhilef, S., Saidur, R., 2018. Improved energy conversion performance of a novel design of concentrated photovoltaic system combined with thermoelectric generator with advance cooling system. *Energy Convers. Manag.* 177, 19–29. <https://doi.org/10.1016/j.enconman.2018.09.053>
- Li, K., Bian, H., Liu, C., Zhang, D., Yang, Y., 2015. Comparison of geothermal with solar and wind power generation systems. *Renew. Sustain. Energy Rev.* 42, 1464–1474. <https://doi.org/10.1016/j.rser.2014.10.049>
- Li, K., Garrison, G., Moore, M., Zhu, Y., Liu, C., Home, R., Petty, S., 2019. Experimental Study on the Effects of Flow Rate and Temperature on Thermoelectric Power Generation, in: *PROCEEDINGS, 44th Workshop on Geothermal Reservoir Engineering Stanford University, Stanford, California, February 11-13, 2019 SGP-TR-214*. Stanford Geothermal Workshop, pp. 1–10.
- Lu, B., Meng, X., Tian, Y., Zhu, M., Suzuki, R.O., 2017. Thermoelectric performance using counter-flowing thermal fluids. *Int. J. Hydrogen Energy* 42, 20835–20842. <https://doi.org/10.1016/j.ijhydene.2017.06.132>
- Lv, S., Liu, X., Liu, M., He, W., Jiang, Q., Hu, Z., Chen, H., 2017. Study of different heat exchange technologies influence on the performance of thermoelectric generators. *Energy Convers. Manag.* 156, 167–177. <https://doi.org/10.1016/j.enconman.2017.11.011>
- Ming, T., Yang, W., Huang, X., Wu, Y., Li, X., Liu, J., 2017. Analytical and numerical investigation on a new compact thermoelectric generator. *Energy Convers. Manag.* 132, 261–271. <https://doi.org/10.1016/j.enconman.2016.11.043>
- Negash, A., 2017. Direct contact thermoelectric generator (DCTEG): A concept for removing the contact resistance between thermoelectric modules and heat source. *Energy Convers. Manag.* 142, 20–27. <https://doi.org/10.1016/j.enconman.2017.03.041>
- Remeli, M.F., Date, A., Orr, B., Ding, L.C., Singh, B., Affandi, N.D.N., Akbarzadeh, A., 2016. Experimental investigation of combined heat recovery and power generation using a heat pipe assisted thermoelectric generator system. *Energy Convers. Manag.* 111, 147–157. <https://doi.org/10.1016/j.enconman.2015.12.032>
- Sajid, M., Hassan, I., Rahman, A., 2017. An overview of cooling of thermoelectric devices. *Renew. Sustain. Energy Rev.* 78, 15–22. <https://doi.org/10.1016/j.rser.2017.04.098>
- Tu, Y., Zhu, W., Lu, T., Deng, Y., 2017. A novel thermoelectric harvester based on high-performance phase change material for space application. *Appl. Energy* 206, 1194–1202. <https://doi.org/10.1016/j.apenergy.2017.10.030>
- Twaha, S., Zhu, J., Yan, Y., Li, B., 2016. A comprehensive review of thermoelectric technology: Materials, applications, modelling and performance improvement. *Renew. Sustain. Energy Rev.* 65, 698–726. <https://doi.org/10.1016/j.rser.2016.07.034>
- Wang, T., Luan, W., Wang, W., Tu, S.T., 2014. Waste heat recovery through plate heat exchanger based thermoelectric generator system. *Appl. Energy* 136, 860–865. <https://doi.org/10.1016/j.apenergy.2014.07.083>
- White, L. V., 2019. Increasing residential solar installations in California: Have local permitting processes historically driven differences between cities? *Energy Policy* 124, 46–53. <https://doi.org/10.1016/j.enpol.2018.09.034>
- Yu, J., Zhao, H., 2007. A numerical model for thermoelectric generator with the parallel-plate heat exchanger. *J. Power Sources* 172, 428–434. <https://doi.org/10.1016/j.jpowsour.2007.07.045>
- Zhang, T., 2016. New thinking on modeling of thermoelectric devices. *Appl. Energy* 168, 65–74. <https://doi.org/10.1016/j.apenergy.2016.01.057>

Zhao, Y., Wang, S., Ge, M., Liang, Z., Liang, Y., Li, Y., 2018. Performance analysis of automobile exhaust thermoelectric generator system with media fluid. *Energy Convers. Manag.* 171, 427–437. <https://doi.org/10.1016/j.enconman.2018.06.006>